Photoproduction and Decay of Light Mesons in CLAS

CLAS Analysis Proposal

M.J. Amaryan (spokesperson),[1,*] Ya. Azimov,[2] M. Battaglieri,[3] W.J. Briscoe,[4] V. Crede,[5] R. De Vita,[3] C. Djalali,[6] M. Dugger,[7] G. Gavalian,[1] S. Ghosh,[8] F. Goldenbaum,[9,10] L. Guo,[11,12] H. Haberzettl,[4] C.E. Hyde,[1] D.G. Ireland,[13] F. Klein,[14] B. Kopf,[15] B. Kubis,[16] A. Kubarovsky,[17,18] V. Kubarovsky,[12] M.C. Kunkel,[1] B. McKinnon,[13] K. Nakayama,[19] C. Nepali (spokesperson),[1] E. Pasyuk,[12] M.V. Polyakov,[20,2] A. Roy,[8] B.G. Ritchie,[7] J. Ritman,[9,10,15] C. Salgado,[21] S. Schadmand (spokesperson),[9,10] S.P. Schneider,[16] I. Strakovsky,[4] D. Weygand,[12] U. Wiedner,[15] and A. Wirzba[9,10,22]

[1] *Old Dominion University, Norfolk, Virginia 23529*
[2] *Petersburg Nuclear Physics Institute, Gatchina, St. Petersburg 188300, Russia*
[3] *INFN, Sezione di Genova, 16146 Genova, Italy*
[4] *The George Washington University, Washington, DC 20052*
[5] *Florida State University, Tallahassee, Florida 32306*
[6] *University of South Carolina, Columbia, South Carolina 29208*
[7] *Arizona State University, Tempe, Arizona 85287-1504*
[8] *Indian Institute of Technology Indore, Khandwa Road, Indore-452017, Madhya Pradesh, India*
[9] *Institut für Kernphysik, Forschungszentrum, Jüelich, Germany*
[10] *Jülich Center for Hadron Physics, Forschungszentrum Jülich, 52425 Jüich, Germany*
[11] *Florida International University, Miami, Florida 33199*
[12] *Thomas Jefferson National Accelerator Facility, Newport News, Virginia 23606*
[13] *University of Glasgow, Glasgow G12 8QQ, United Kingdom*
[14] *Catholic University of America, Washington, DC 20064*
[15] *Institut für Experimentalphysik I, Ruhr Universität Bochum, 44780 Bochum, Germany*
[16] *Helmholtz-Institut für Strahlen- und Kernphysk (Theorie) and Bethe Center for Theoretical Physics, Universität Bonn, D-53115 Bonn, Germany*
[17] *Rensselaer Polytechnic Institute, Troy, New York 12180-3590*
[18] *Skobeltsyn Nuclear Physics Institute, 119899 Moscow, Russia*
[19] *Department of Physics and Astronomy, University of Georgia, Athens, GA 30602, USA*
[20] *Institut für Theoretische Physik II, Ruhr–Universität Bochum, D–44780 Bochum, Germany*
[21] *Norfolk State University, Norfolk, VA 23504, USA*
[22] *Institute for Advanced Simulation, Forschungszentrum Jülich, 52425 Jülich, Germany*

(Dated: December 24, 2012)

*Electronic address: mamaryan@odu.edu; Contact person.

Contents

I. INTRODUCTION

Low energy Quantum Chromodynamics (QCD) is responsible for the binding of hadrons and for the mass of the visible universe. A unique way to explore low energy QCD is by measuring the decays of light mesons, specifically the π^0, η and η' pseudoscalar mesons and light vector mesons ρ, ω, ϕ. In particular, the η and η' mesons present important information on the low energy dynamics of QCD: the mechanism of spontaneous chiral symmetry breaking and the $U_A(1)$ anomaly. The importance of this topic is shown by the number of experiments performed at an impressive array of facilities including KLOE, CLEO, BES, MAMI, Bonn, COSY, BABAR, BELLE, and CERN. We have recently shown that CLAS photoproduction data has superior statistics in many channels, exceeding that of published results by a factor of up to ten.

Close to the zero-energy limit of the spontaneous breaking of chiral symmetry, chiral perturbation theory (ChPT) and, more generally, effective field theories, incorporate the symmetries of QCD while avoiding the tremendous calculational difficulties of the full theory in the non-perturbative regime. Comparisons of ChPT predictions with high statistics data on the branching ratios and decay distributions of light mesons will provide insight into the non-perturbative regime of strong interactions and provide important information for a firmer foundation of hadronic physics rooted in the standard model.

II. PSEUDOSCALAR MESONS

Below we outline a physics program to explore light meson decays measured in the CLAS g11 and g12 hydrogen photoproduction experiments. Preliminary analyses of these data show that CLAS data can have a major impact on studies of light meson decays measured in other facilities and is independent of the production vertex. Experimental data are presented with emphasis on the photoproduction reactions

$$\gamma + p \to p + \begin{cases} \pi^0 \\ \eta \\ \eta' \end{cases} \tag{1}$$

collected in the following decay modes:

- Dalitz decays: π^0, η, or $\eta' \to e^+e^-\gamma$
- Radiative decays: η or $\eta' \to \pi^+\pi^-\gamma$
- Hadronic decays: η or $\eta' \to \pi^+\pi^-\pi^0$ and $\eta' \to \pi^+\pi^-\eta$

In order to fully exploit this rich vein of data and to cast more light on low energy QCD, dedicated efforts and sufficient manpower is needed to complete the analyses and publish these results.

1. Dalitz decays

The branching ratios for radiative decay of pseudoscalar mesons π^0 and η have been measured and are recorded by the PDG [1], however there is only an upper limit quoted for $\eta' \to e^+e^-\gamma$.

In this proposal we briefly present our preliminary distribution of the $e^+e^-\gamma$ invariant mass from CLAS photoproduction data. This is a H$(\gamma, pe^+e^-\gamma)$X four-fold coincidence event sample with an upper bound on the missing energy.

Peaks of π^0, η and η' are shown separately, with fitted positions corresponding to their PDG values. In addition, there is a clear signal in the ρ-ω region, and a small peak at the ϕ-mass. With a branching ratio of $(1.174 \pm 0.035)\%$, the three body decay $\pi^0 \to e^+e^-\gamma$ is the second most important decay channel of the neutral pion and is deeply connected to the main decay mode $\pi^0 \to \gamma\gamma$ ($Br = 98.823 \pm 0.034\%$) with anomalous $\pi^0 - \gamma - \gamma$ vertex. Significant interest to the Dalitz decay of π^0 lies in the fact that it provides information on the semi off-shell $\pi^0 - \gamma - \gamma^*$ transition form factor $F_{\pi^0\gamma\gamma^*}(q^2)$ in the time-like region, and more specifically on its slope parameter a_π. The determinations of a_π obtained from the differential decay rate of Dalitz decay

$$a_\pi = -0.11 \pm 0.03 \pm 0.08 \text{ [2]}$$
$$a_\pi = +0.026 \pm 0.024 \pm 0.0048 \text{ [3]}$$
$$a_\pi = +0.025 \pm 0.014 \pm 0.026 \text{ [4]}$$

Here a_π is defined from the following expression for the decay rate [5]

$$\frac{d\Gamma(\pi^0 \to e^+e^-\gamma)}{dx\Gamma(\pi^0 \to \gamma\gamma)} = (\frac{d\Gamma}{dx})_{QED} \times |F(x)|^2$$
$$(\frac{d\Gamma}{dx})_{QED} = \frac{2\alpha}{3\pi}\frac{1}{x}(1-x)^3(1+\frac{r}{2x})(1-\frac{r}{x})^{1/2}$$
$$F(x) = 1 + a_\pi x$$

where $x = m^2_{e^+e^-}/m^2_{\pi^0}$, $r = 4m^2_e/m^2_{\pi^0}$, and $F(x)$ is π^0 transition form factor.
These measurements have large error bars, as compared to the values extracted from the extrapolation of data at higher energies in the space-like region, $Q^2 = -q^2 > 0.5GeV^2$, obtained by CELL0 and CLEO collaborations,

$$a_\pi = +0.0326 \pm 0.0026 \pm 0.0026 \text{ [6]}$$
$$a_\pi = +0.0303 \pm 0.0008 \pm 0.0009 \pm 0.0012 \text{ [7]}$$

Experimental data from CELLO [6] , CLEO [7] and BABAR [8] experiments are presented in Fig. 1. Extraction of a_π from these data is model dependent and a direct and accurate determination of a_π from the decay $\pi^0 \to e^+e^-\gamma$ would offer very important source of information to understand transition form factor of neutral pion. Another reason for the importance of this information is related to the precise determination of the most uncertain light-by-light radiative corrections to the anomalous magnetic moment of the muon, a_μ, measured in g-2 experiment [9].

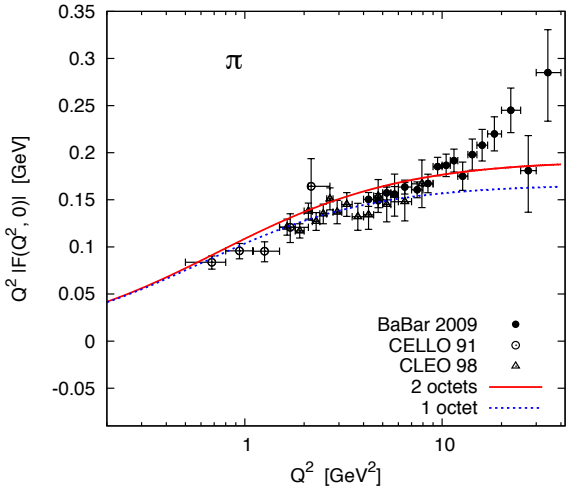

FIG. 1: Experimental data on $F(Q^2, 0)$ from the reaction $e^+e^- \to \pi^0$ obtained by CELLO, CLEO and BABAR experiments with one of recent theoretical prediction from [10].

In Fig. 2 we present invariant mass $M(e^+e^-\gamma)$ from the reaction $\gamma p \to pe^+e^-\gamma$ on hydrogen target obtained from data collected by the g12 experiment. One can see clear peaks of π^0, η, η', but also peaks of ω and ϕ vector mesons from the decay $e^+e^-\pi^0$, when one of photons from π^0 decay was missing. This spectrum is obtained by cutting on the missing mass and missing energy of all detected particles restricting possibility of π^0 production, however due to the detector resolution it can not be completely suppressed. In Fig. 3 we show each of π^0, η, η' peaks from Fig. 2 with a fit with Gaussian and second order polynomial function. As one can see we have very clean signal of π^0 and η mesons. The reconstructed for the first time η' peak in this decay mode will allow to measure relative branching ratio of this mode to $\eta' \to \eta\pi^+\pi^-$. Systematic error of such a measurement has to be evaluated in detail at more advanced stage of the analysis, however there is no reason to expect this to be significantly different from the systematic errors of a few per cent in the measurement of photoproduction cross section of η' measured by the CLAS collaboration.

New experiment is proposed in KLOE-2 [10] to measure $F_{\pi^0}(Q^2, 0)$ with statistical precision shown in Fig. 4 (left panel). Statistically significant data are already collected with CLAS. The CLAS g12 raw data under the π^0 peak in $e^+e^-\gamma$ decay mode are presented in Fig. 4 (right panel), which will allow to extract the slope of Q^2 dependence, a_{π^0}, in the time-like region at very low Q^2 with statistical accuracy for the first time comparable or better than that extracted from $e^+e^- \to \pi^0$ data at higher Q^2 in space-like region.

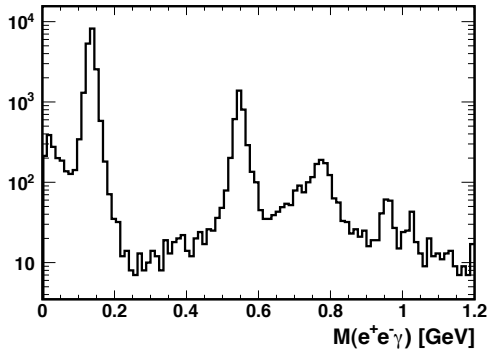

FIG. 2: The $e^+e^-\gamma$ invariant mass distribution in the reaction $\gamma p \to pe^+e^-\gamma$.

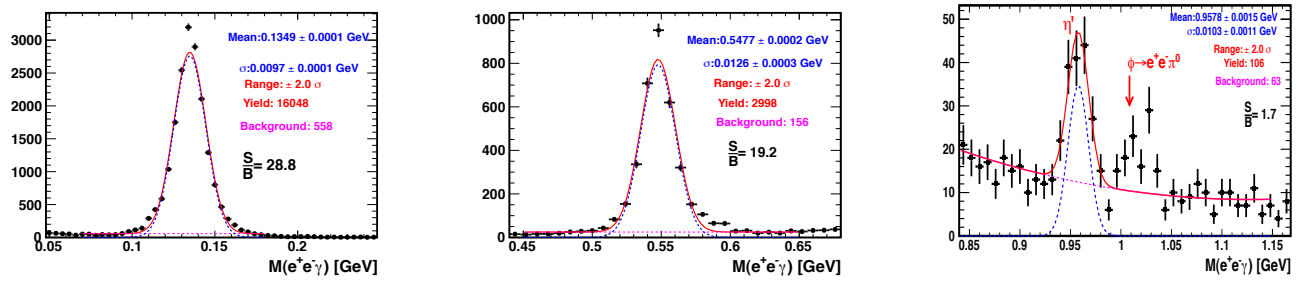

FIG. 3: Invariant mass, $M(e^+e^-\gamma)$, distribution for different regions from Fig. 2. Left panel: peak of π^0, middle panel: peak of η, right panel: peak of η'.

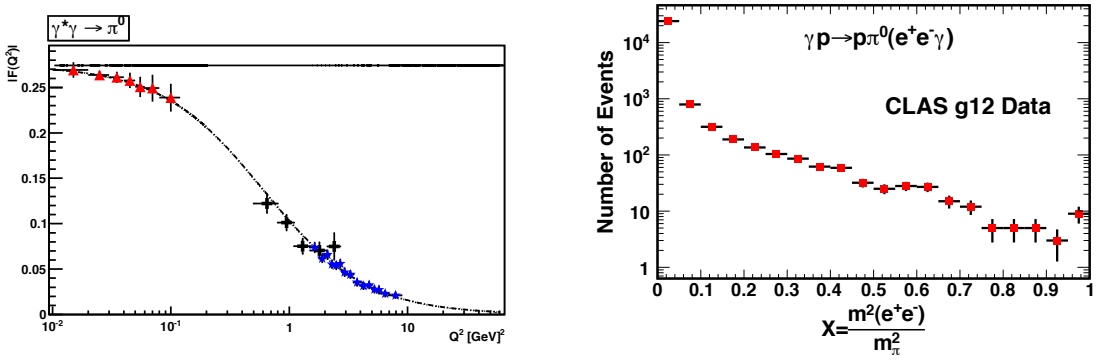

FIG. 4: Left panel: experimental data from CELLO (black crosses) and CLEO (blue stars) at low Q^2 together with KLOE-2 proposal (red triangles) to measure $F_{\pi^0}(Q^2, 0)$ at very low Q^2 [10]. Dashed line is the $F(Q^2)$ form factor according to LMD+V model [39], solid line is $F(0)$ given by Wess-Zumino-Witten term. Right panel: raw data from CLAS g12 experiment within 2σ of the peak of π^0 from Fig. 3 (left panel), plotted vs the ratio $X = \frac{m^2_{e^+e^-}}{m^2_\pi}$.

One of the important questions is identification of pseudoscalar mesons in Dalitz decay mode $e^+e^-\gamma$. As one can see from Fig. 5, left panel, after restricting missing energy $|ME - E_\gamma|$ <0.05GeV, where $ME = E^{beam}_\gamma + M_p - E_p - E_{e^+} - E_{e^-} - E_\gamma$, we observe a single photon peak in $M^2_X(pe^+e^-\gamma)$. On the right panel of the same figure we plot missing mass $M^2_X(pe^+e^-)$ here with an additional cut cut on $|M^2_X(pe^+e^-\gamma)| < 0.01\text{GeV}^2$. As one can see again we have single photon peak only. Therefore the contribution from $\omega \to e^+e^-\pi^0$ is excluded either in the invariant mass $M(e^+e^-\gamma)$ or missing mass $M_X(p)$. On the other hand as e^+e^- mass distribution spans from the threshold, the decay

$\eta' \to \omega\gamma$ (BR=2.75%) can not be of major concern and is irrelevant.

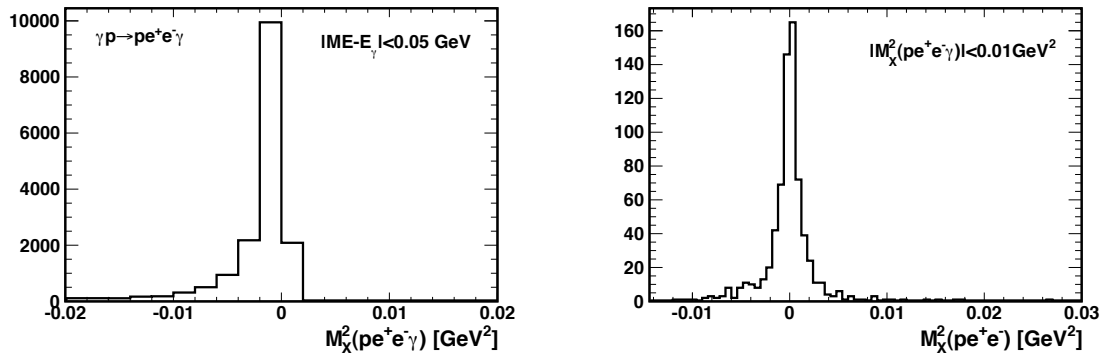

FIG. 5: Left panel: missing mass squared $M_X^2(pe^+e^-\gamma)$ of all detected final state particles with the cut on missing energy $|ME - E_\gamma|$ <0.05GeV. Right panel: missing mass $M_X^2(pe^+e^-)$ with additional cut $|M_X^2(pe^+e^-\gamma)| < 0.01\text{GeV}^2$.

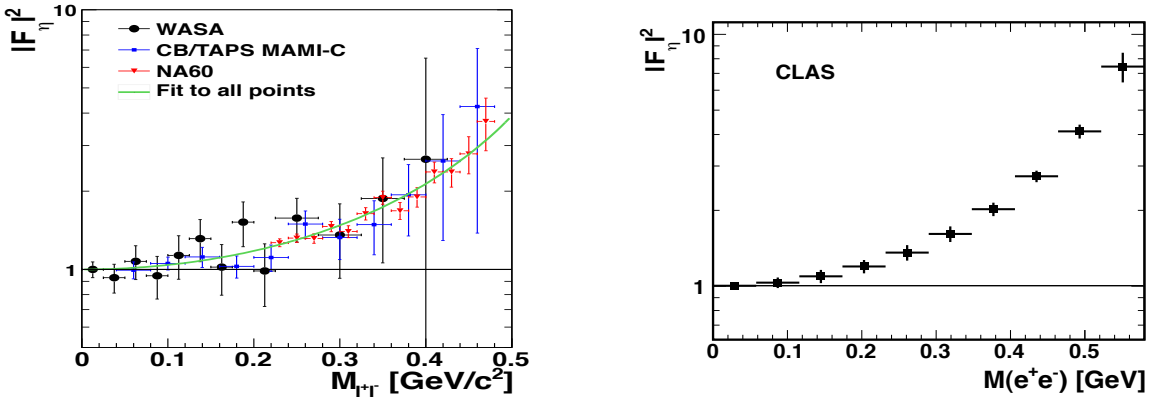

FIG. 6: Left panel: Experimental spectrum of the squared transition form factor, $|F_\eta|^2$, as a function of $M(l^+l^-)$. The green, solid line is the fit to all experimental points. The black, solid line is the QED model assumption of a point-like meson. Right panel: projected form factor with statistical errors obtained from CLAS g12 experiment within 2σ of the peak of η from Fig. 3 (middle panel), plotted vs $M(e^+e^-)$.

In Fig. 6 left panel we present world data on η form factor, on the right panel we present projected form factor with statistical errors obtained from CLAS g12 experiment within 2σ of the peak of η. This CLAS dataset for the η Dalitz decay exceeds by several times the statistics of the recent MAMI CB/TAPS [11], and NA60 dimuon ($\eta \to \mu^+\mu^-\gamma$) [12] measurements. Both of these results observe a clear deviation of the form factor from the simple QED result based on the $\eta \to \gamma\gamma$ matrix element. The CLAS data can significantly improve the extraction of the form factor over the full accessible range $0 < m_{e^+e^-} \leq m_\eta$, including the region below twice the muon mass, which is inaccessible in the NA60 experiment.

2. Radiative decays

The two photon decays of pseudoscalar mesons $\pi^0, \eta, \eta' \to \gamma\gamma$ are understood as proceeding from the so-called triangle or axial anomaly, Fig. 7 (left panel), while radiative decays of $\eta(\eta') \to \pi^+\pi^-\gamma$ are related to the so-called box anomaly, Fig. 7 (right panel).

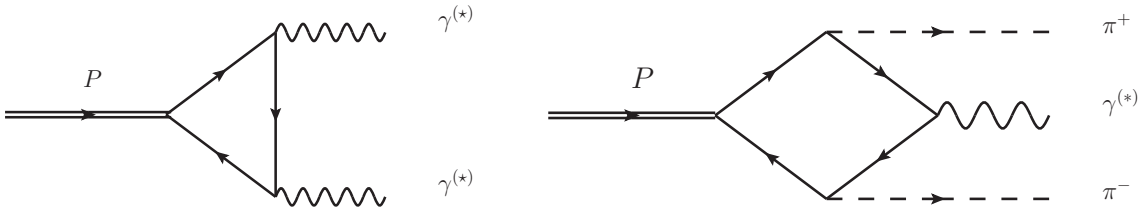

FIG. 7: Left panel: triangle anomaly. Right panel: box anomaly.

The box anomaly determines the $\eta(\eta') \to \pi^+\pi^-\gamma$ widths in the chiral limit, as it is described in Ref. [13] with a comprehensive theoretical analysis of the photon energy distribution of the radiative decay of the η and η' mesons. These decays provide an important test of the box anomaly, which also describes the $\gamma\pi^+\pi^-\pi^0$ (VAAA) vertex in the chiral limit, with the effects of η_0 and η_8 mixing.

As in case of Dalitz decay the decay of pseudoscalar meson to $\pi^+\pi^-\gamma$ requires identification of final state and separation of single photon from π^0. In Fig. 8 we first present missing mass of all detected particles with a cut on missing energy $|ME - E_\gamma| < 0.05$GeV. This plot shows a peak around zero, but it doesn't yet secure rejection of π^0 in the event, as it could have been one low energy photon from the decay missing and it will mimic single photon production. To make sure if there is a π^0 except of $p, \pi^+\pi^-$ in the final state in Fig. 9 upper row we plot missing mass $M(p\pi^+\pi^-)^2$ with additional cut $M(p\pi^+\pi^-\gamma)^2$ <0.01 GeV^2 for different ranges of missing mass $M_X(p)$ in the range of $\eta, \rho/\omega, \eta'$. As one can see we have very clear peaks of single γ and π^0, the latter being more significant in the region of ω because of very strong $\omega \to \pi^+\pi^-\pi^0$ decay. In the lower panel of the same figure we plot invariant mass $M(\pi^+\pi^-\gamma$ (red histogram) and missing mass $M_X(p)$ (black histogram). As one can see all particles are reconstructed in both cases, however missing mass has better resolution.

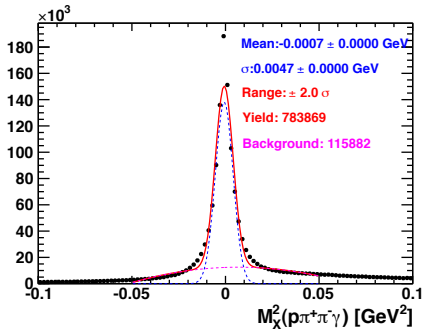

FIG. 8: Missing mass $M_X(p\pi^+\pi^-\gamma)$ of all detected final state particles.

In Fig. 10 the cm photon energy distribution, E_γ^{cm} is presented for η (left panet) and η' (right panel). Experimental data are from the following experiments [14–16]). Error weighted fits are performed in [13]. The decay rate of $\eta(\eta') \to \pi^+\pi^-\gamma$ in [13] is presented as

$$\frac{d\Gamma}{ds_{\pi\pi}} = |AP(s_{\pi\pi})F_V(s_{\pi\pi})|^2\Gamma_0(s_{\pi\pi}), \tag{2}$$

where A is a normalization parameter and $\Gamma_0(s_{\pi\pi})$ collects phase-space terms and the kinematics of the absolute square of the simplest gauge invariant matrix element (for point-like particles). Here $s_{\pi\pi} = m^2 - 2E_\gamma m$ is squared

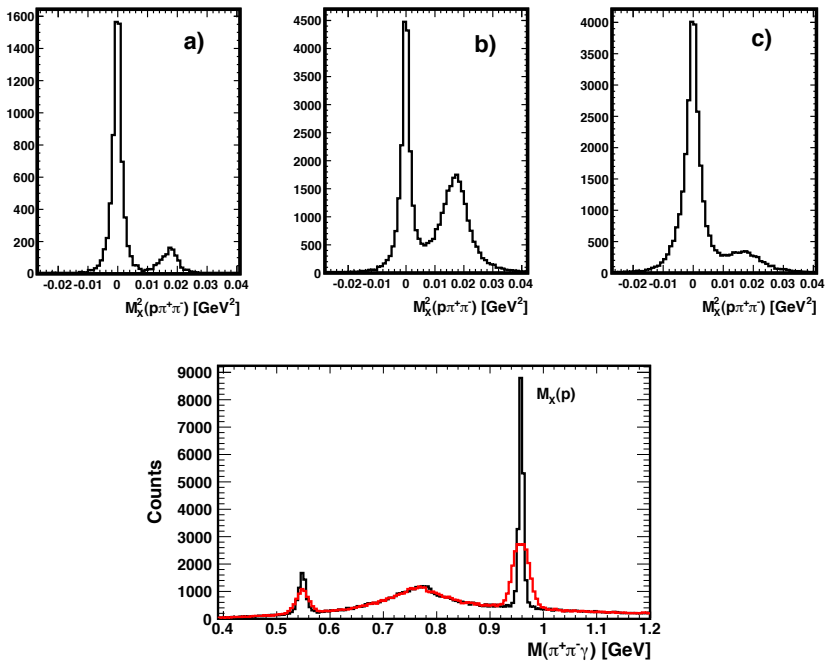

FIG. 9: Upper row is a distribution of events vs missing mass squared $M_X^2(p\pi^+\pi^-)$ for the range: a) $M_X(p) = 0.55 \pm 0.02$ GeV; b) $M_X(p) = 0.76 \pm 0.06$ GeV; c) $M_X(p) = 0.96 \pm 0.02$ GeV. Lower row is a distribution of invariant mass $M(\pi^+\pi^-\gamma)$ (red histogram) and missing mass $M_X(p)$ with the cuts: $M_X^2(p\pi^+\pi^-\gamma) < 0.01\text{GeV}^2$ $M_X^2(p\pi^+\pi^-) < 0.005\text{GeV}^2$.

invariant mass of two-pions system, m is the mass of parent particle and E_γ is the photon energy in the rest frame of $\eta(\eta')$. The pion form factor $F_V(s_{\pi\pi})$ is well known from direct measurements of $e^+e^- \to \pi^+\pi^-$. On the other hand, the function $P(s_{\pi\pi})$ is reaction specific and is expected to be perturbative in the sense of Chiral Perturbation Theory. This function can be expanded as

$$P(s_{\pi\pi}) = 1 + \alpha s_{\pi\pi} + O(s_{\pi\pi}^2) \tag{3}$$

The following slope parameter values for η and η' are extracted from the fits in Fig. 10

$$\alpha = (2.01 \pm 0.26) GeV^{-2}; \qquad \alpha' = (2.28 \pm 0.56) GeV^{-2}. \tag{4}$$

These can then be interpreted via a matching to oneloop U(3) extended ChPT as well as a comparison to earlier studies.

Existing CLAS data can significantly improve statistical precision of these parameters. In Fig. 11 (upper panel) the missing mass of the proton from the CLAS g11 dataset is presented for the exclusive reaction $\gamma + p \to p\pi^+\pi^-\gamma$. In both the η and η' peaks, the statistics is more than an order of magnitude higher than existing world data. *The g12 experiment provides additionally three times more statistics in this channel.* In Fig. 11 lower panels, the photon energy distributions from the $\pi^+\pi^-\gamma$ decays of η and η', respectively, are presented in the center-of-mass frame of the parent. This analysis of high statistics CLAS data will decrease statistical uncertainty of slope parameters $\alpha(\alpha')$ to the per cent level providing an unprecedented test of ChPT, including the effects of mixing of the $SU(3)$ singlet and octet η states.

In the spectrum of Fig. 11 (upper panel) we might possibly see a hint of ρ-ω interference. Although the $\rho \to \pi^+\pi^-\gamma$ branching ratio is known to 15% precision, only an upper bound for the ω is quoted in the PDG [1]. This channel may also yield new results, in particular a measurement of $\omega \to \pi^+\pi^-\gamma$ branching ratio. Similar studies are performed with $\rho, \omega \to e^+e^-$ decay in CLAS (M.H. Wood et al., "Absorption of ω and ϕ Mesons in Nuclei". The paper CLAS collaboration review is in progress), where clear overlap of ρ and ω mesons in this decay mode is observed.

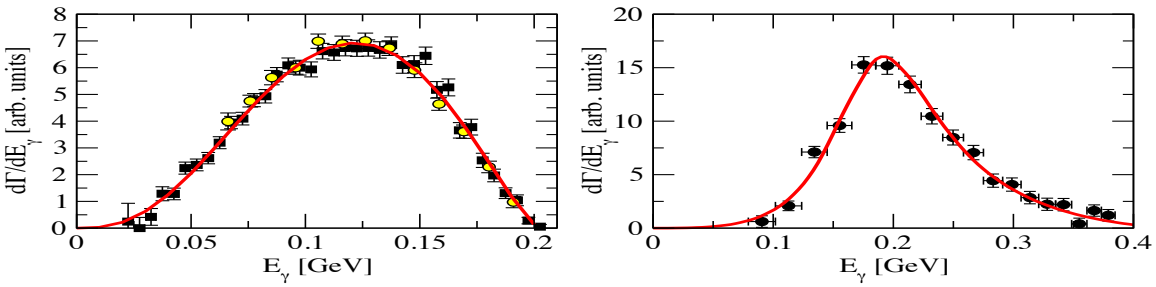

FIG. 10: Left panel: distribution of E_γ in cm frame of *eta*. Right panel: same for η'. Experimental data are from [14–16]. Error weighted fits are performed in [13].

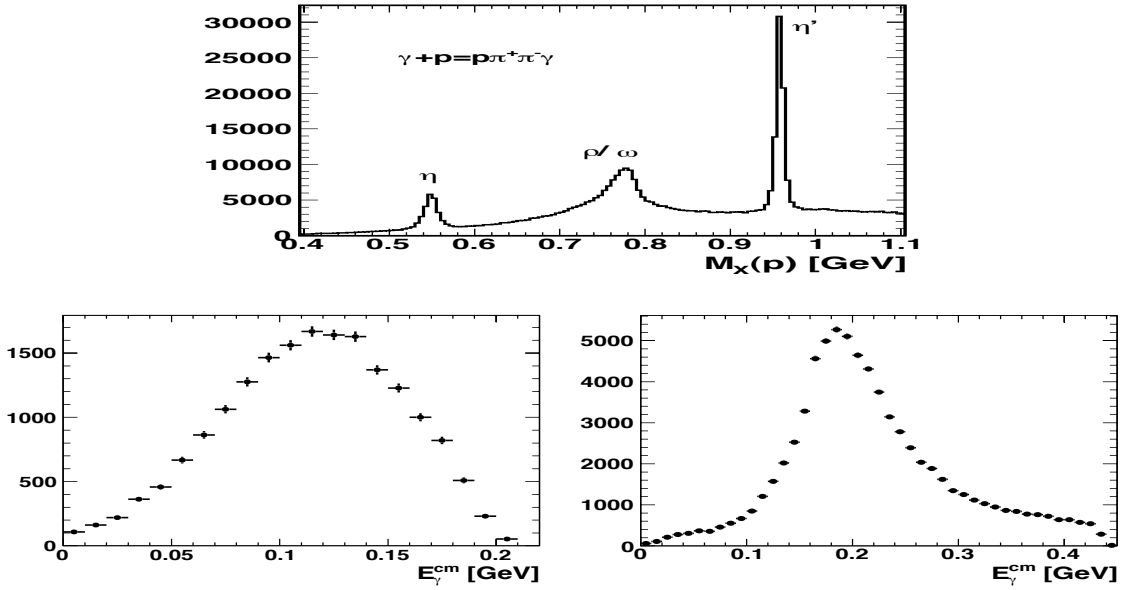

FIG. 11: Upper panel: distribution of the missing mass of the proton (mass of $\pi^+\pi^-\gamma$ system) in the exclusive reaction $\gamma + p \to p\pi^+\pi^-\gamma$. Lower left panel: the γ energy distribution in the η cm frame. Right panel: same as left panel plotted for the η' decay. All three plots show raw number of events from CLAS g11 experiment before the acceptance and efficiency corrections.

3. Hadronic decays

In this section we present experimental data for the reaction

$$\gamma + p \to p\pi^+\pi^- \left\{ \begin{array}{c} \pi^0 \\ \eta \end{array} \right. . \tag{5}$$

The π^0 or η is identified via missing mass of the $\mathrm{H}(\gamma, p\pi^+\pi^-)X$ reaction.

To get an idea about how missing mass of all detected particles look like in Fig. 12 we plot $M_X(p\pi^+\pi^-)$ for different ranges of missing mass of proton $M_X(p) = \eta, \omega, \eta'$ in a ± 0.02 GeV window of corresponding peaks.

In Fig. 13 (left panel) a distribution of missing mass of the proton in the $\gamma + p \to p\pi^+\pi^-\pi^0$ reaction is presented showing clear peaks for the η and ω mesons with $\sim$2M and $\sim$20M events in the peaks, respectively

There are also hints of η' and ϕ mesons. To see the η' and ϕ signals, in Fig. 13 (right panel) we plot a zoom of the same distribution in the mass range above the ω meson. We clearly observe one of the rare decays $\eta' \to \pi^+\pi^-\pi^0$ ($\mathrm{Br} = 3.6 \pm 0.1 \times 10^{-3}$) and the OZI violating decay $\phi \to \pi^+\pi^-\pi^0$ (Br=15.3%). This is the first observation of these

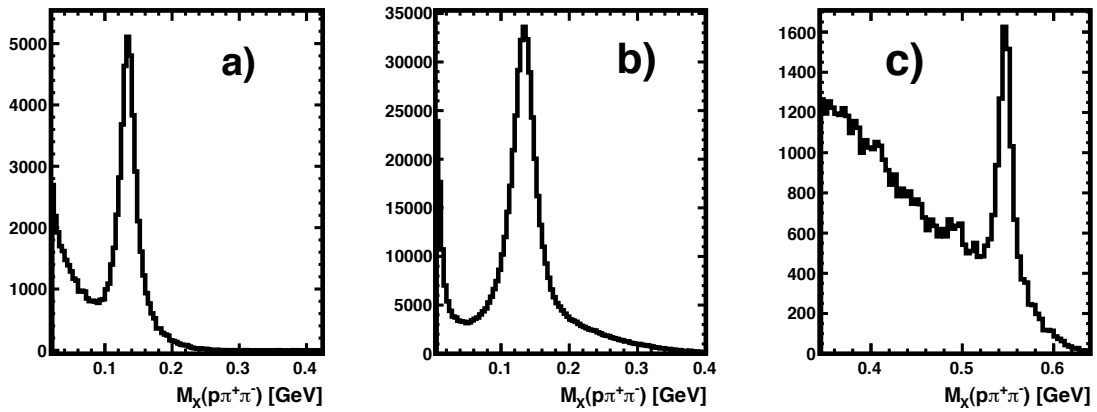

FIG. 12: Missing mass $M_X(p\pi^+\pi^-)$: a) for $|M_X(p) - 0.55|$ <0.02 GeV; b) $|M_X(p) - 0.78|$ <0.02 GeV; and c) $|M_X(p) - 0.96|$ <0.02 GeV.

decays in photoproduction. According to Gross, Treiman, and Wilczek [17], the decay width ratio:

$$\frac{\Gamma(\eta' \to \pi^0\pi^+\pi^-)}{\Gamma(\eta' \to \eta\pi^+\pi^-)} \propto \left[\frac{m_d - m_u}{m_s}\right]^2 \tag{6}$$

is sensitive to the quark mass difference $m_d - m_u$, where m_d. m_u, and m_s are masses of u, d and s quarks respectively.

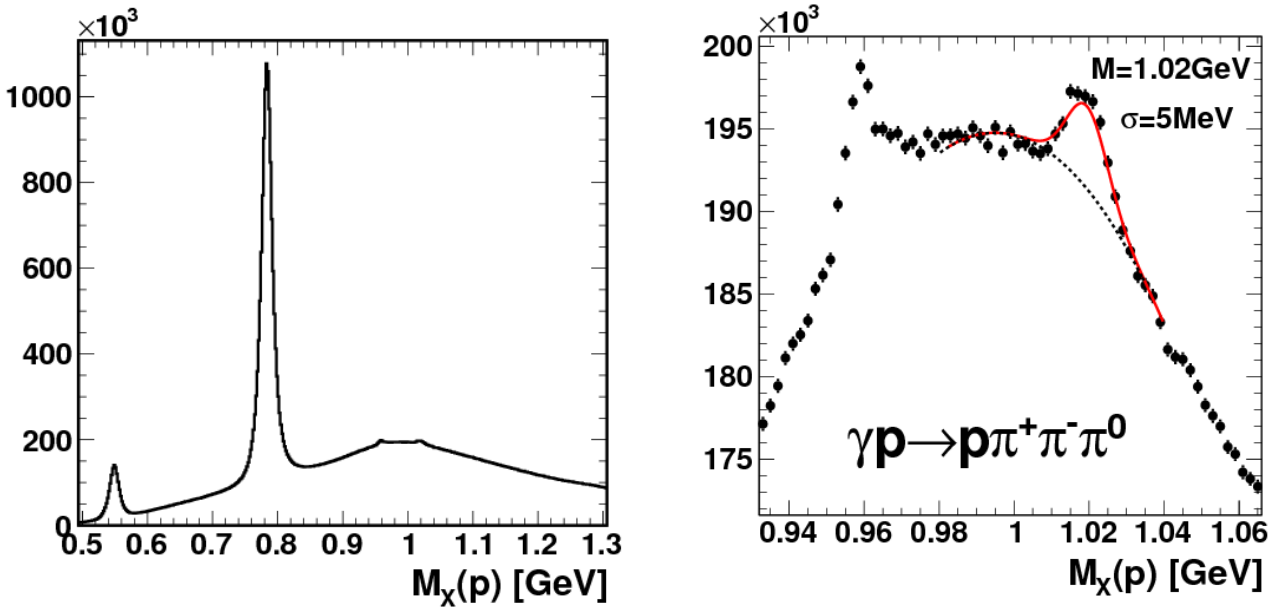

FIG. 13: Left panel: distribution of missing mass of the proton in the reaction $\gamma + p \to p\pi^+\pi^-\pi^0$. Right panel: the same for the range of invariant mass above ω meson production. Experimental data are from CLAS g11 experiment.

Our Dalitz plot distribution for the decay $\eta \to \pi^+\pi^-\pi^0$ is seen in Fig. 14 with x and y distributions. As one can see the CLAS data have a full coverage in these variables.

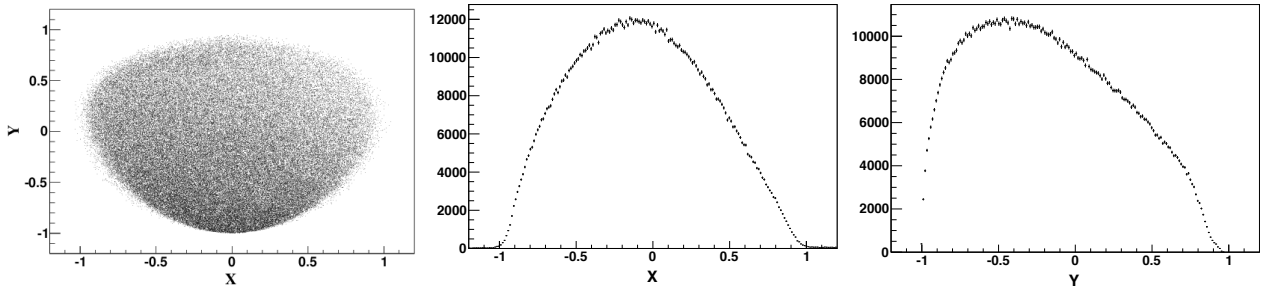

FIG. 14: Left panel: Dalitz plot distribution of the decay $\eta \to \pi^+\pi^-\pi^0$. Middle panel: x-projection of the Dalitz plot. Right panel: y-projection of the Dalitz plot. Experimental data are from CLAS g11 experiment.

In Fig. 15 (left panel) we present the distribution of missing mass of the proton in the reaction $\gamma + p \to p\pi^+\pi^-\eta$, where η is reconstructed in the missing mass of the $p\pi^+\pi^-$ system, i.e. $\gamma(^1H, p\pi^+\pi^-)X$. As one can see there is a clear peak of η' with ∼300K events, which is almost an order of magnitude higher than the recent BES [18] data. In Fig. 16 we show our Dalitz plot distribution for the decay $\eta' \to \pi^+\pi^-\eta$.

The internal dynamics of the decay $\eta \to \pi^+\pi^-\pi^0$ and $\eta' \to \pi^+\pi^-\eta$ can be described by two degrees of freedom since all particles involved have spin zero. The Dalitz plot distribution for the decay $\eta \to \pi^+\pi^-\pi^0$ is described by the following two variables:

$$X = \frac{\sqrt{3}}{Q}(T_{\pi^+} - T_{\pi^-}), \qquad Y = \frac{3T_{\pi^0}}{Q} - 1, \tag{7}$$

where T_π is the kinetic energy of the meson in the η rest frame and $Q = T_{\pi^+} + T_{\pi^-} + T_{\pi^0}$.

The corresponding variables for the decay $\eta' \to \pi^+\pi^-\eta$ are

$$X = \frac{\sqrt{3}}{Q}(T_{\pi^+} - T_{\pi^-}), \qquad Y = \frac{m_\eta + 2m_\pi}{m_\pi}\frac{T_\eta}{Q} - 1, \tag{8}$$

here $Q = T_{\pi^+} + T_{\pi^-} + T_\eta$

The matrix element of the decay can be expanded around the center of the corresponding Dalitz plot in order to obtain the Dalitz slope parameters:

$$M^2 = A(1 + aY + bY^2 + cX + dX^2), \tag{9}$$

where a, b, c and d are real parameters and A is a normalization factor. Our high statistics dataset will allow us to extract these polynomial coefficients with the high statistical precision as it is presented in the fifth column of Table I based on CLAS data from g11 experiment only (see Fig. 17). An addition of g12 data will reduce these errors by another factor of two.

At the ϕ mass, there is also a hint of the G-parity violating decay mode: $\phi \to \pi^+\pi^-\eta$. In Fig. 15 (right panel) we show a zoom of the mass distribution in the region of the ϕ, showing a small peak at the ϕ mass. This decay mode has never been observed, PDG quotes only an upper limit for the branching ratio: Br $< 1.8 \times 10^{-5}$. The theoretical model [19] predicts an signifacantly smaller branching on the order of $\sim 3 \times 10^{-7}$. A measurement of this branching ratio can have an important impact.

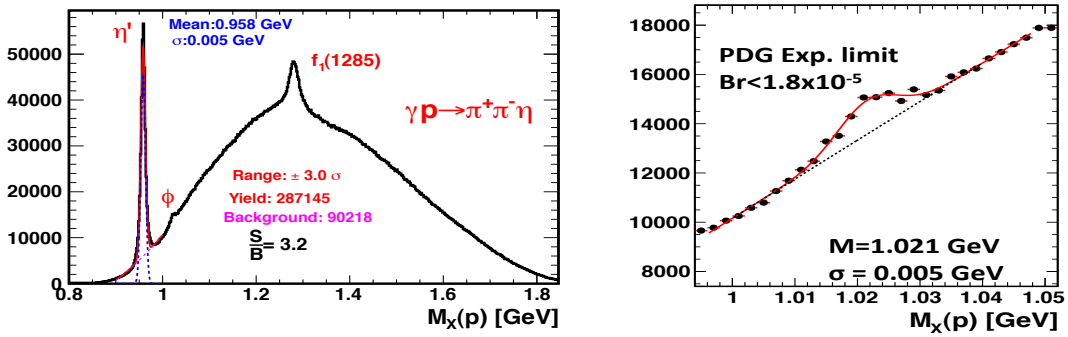

FIG. 15: Left panel: distribution of missing mass of the proton for the reaction $\gamma + p \to p\pi^+\pi^-\eta$. Right panel: zoom of the left figure with the fit of ϕ peak. Experimental data are from CLAS g11 experiment.

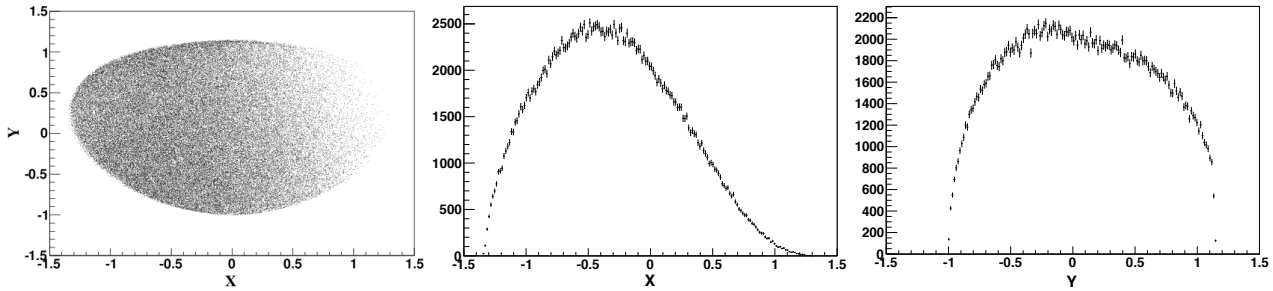

FIG. 16: Left panel: Dalitz plot distribution of the decay $\eta' \to \pi^+\pi^-\eta$. Middle panel: x-projection of the Dalitz plot. Right panel: y-projection of the Dalitz plot. Experimental data are from CLAS g11 experiment.

Par.	VES	Theory	BES	Stat err. In BES	Stat. err. In CLAS
a	-0.127+-0.018	-0.116+-0.011	-0.047+-0.012	+-0.011	+-0.004
b	-0.106+-0.032	-0.042+-0.034	-0.069+-0.021	+-0.019	+-0.006
c	+0.015+-0.018	----------	+0.019+-0.012	+-0.011	+-0.004
d	-0.082+-0.019	+0.010+-0.019	-0.073+-0.013	+-0.012	+-0.004

FIG. 17: Table I: Dalitz plot parameters from experiment and from theory prediction [18]. The fourth column shows statistical error achieved at BES and the fifth column shows expected statistical error from the CLAS g11 data.

III. VECTOR MESONS

A. Dalitz Decay $\omega \to e^+e^-\pi^0$

In Dalitz decays, the vector meson decays into a pseudoscalar meson and a lepton pair, formed by internal conversion of an intermediate virtual photon. In the vector meson dominance (VMD) model, the form factor is the same as measured in the $\pi^0 \to \gamma e^+e^-$ and $\eta \to \gamma e^+e^-$ decays and in the $e^+e^- \to e^+e^-\pi^0$ production processes. The $V \to PSe^+e^-$ decay provides unique information about the form factor in the time-like region where vector particle has an invariant mass squared significantly greater than zero. The knowledge of the π^0 and η form factors is also needed for the interpretation of the g-2 [9] and $\pi^0 \to e^+e^-$ [20–22] experiments. The transition form factor for the ω meson seems to deviate strongly from VMD predictions whereas pseudoscalar meson decays involving dileptons typically agree with VMD, for example, $\pi^0 \to \gamma e^+e^-$ and $\eta \to \gamma\mu^+\mu^-$, [5]. A theoretical explanation for the observed deviation from VMD is in need of improved experimental input and is pursued with current theoretical efforts [23] going beyond VMD in a systematic way. It is important to determine the transition form factors for vector mesons via Dalitz decays with different experimental methods. This measurement will have the highest statistics achieved so

far. In Fig. 18 (left panel) missing mass squared, $M_X^2(pe^+e^-)$ is presented for events under the ω peak. As one can see very narrow peak at zero, corresponding to the $\omega \to e^+e^-$ except of prominent peaks of psudoscalar mesons there is a clear peak of ω meson. The results obtained from the CLAS data can be compared with the results extracted from the heavy-ion NA60 experiment [12] for ω mesons.

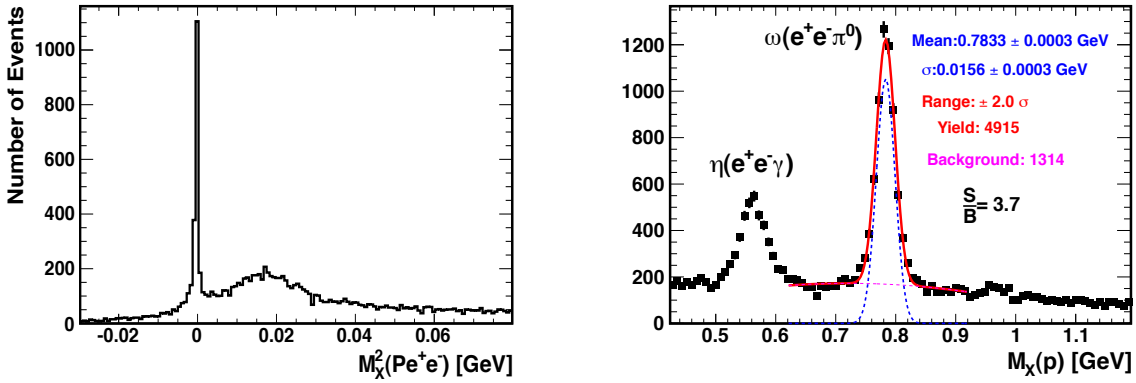

FIG. 18: Left panel: missing mass squared, $M_X^2(pe^+e^-)$, for events within 2σ of the ω peak. Right panel: missing mass of the proton for events under the π^0 peak from the left panel $|M_X^2(pe^+e^-) - M_{\pi^0}^2| < 0.01$ GeV^2.

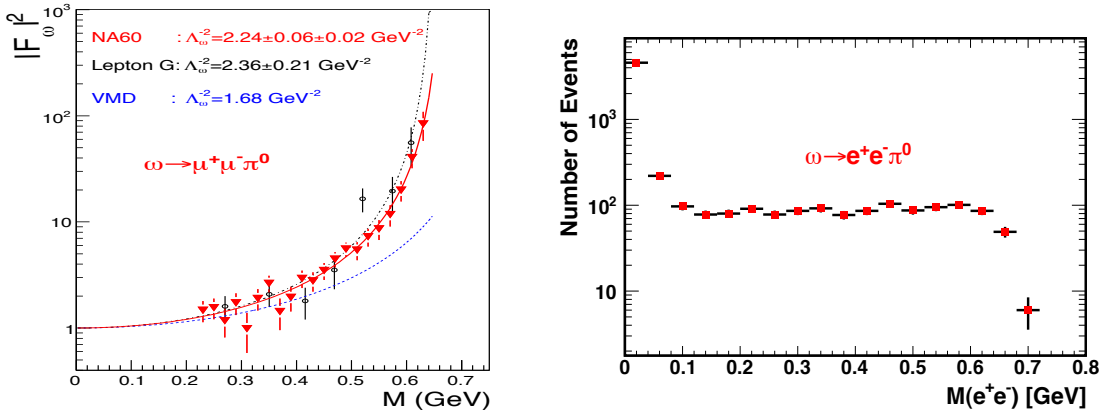

FIG. 19: Left panel: transition form factor of ω from NA60 experiment [12] (red triangles), compared to the previous measurement by the Lepton-G experiment [24] (open circles) and to the expectation from VMD (blue dashed line). The solid red and black dashed-dotted lines are results of fitting the experimental data with the pole dependence $|F^2| = (1 - M^2/\Lambda^2)^{-2}$. Right panel: missing mass of the proton for events under the π^0 peak from the left panel $|M_X^2(pe^+e^-) - M_{\pi^0}^2| < 0.01$ GeV^2 and within 2σ of the ω peak from CLAS g12 Data.

In Fig. 19 (left panel) ω transition form factor extracted from experimental data obtained by Lepton-G [24] and NA60 [12] experiments is presented as a function of the invariant mass of muon pairs. The blue dashed line shows expectation of VMD model which significantly deviates from the fit to experimental data of both experiments. In Fig. 19 (right panel) number of events from the CLAS g12 experiment is presented as a function of invariant mass of electron-positron pairs from the decay $\omega \to e^+e^-\gamma$. It shows that highest statistical precision achieved so far with CLAS data and extends the range of virtuality below two muon mass.

IV. SUMMARY

In conclusion from our preliminary analyses one can see that the CLAS data on photoproduction and decay of light mesons can contribute significantly to essential topics of low energy QCD. The data already on tape at JLab in some of these channels have statistics that is not in a reach of other world facilities. As we tried to underline above, we anticipate at least the following physics results to be released within the scope of presented proposal:

1. Transition form factor of π^0 in the time-like region from Dalitz decay $e^+e^-\gamma$
2. Transition form factor of η in the time-like region from Dalitz decay $e^+e^-\gamma$
3. Branching ratio $\eta' \to e^+e^-\gamma$ for the first time
4. Measurement of E_γ distribution in radiative decay $\eta \to \pi^+\pi^-\gamma$
5. Measurement of E_γ distribution in radiative decay $\eta' \to \pi^+\pi^-\gamma$
6. Transition form factor of ω in time-like region from Dalitz decay $\omega \to e^+e^-\pi^0$
7. Dalitz plot analysis of hadronic decay $\eta \to \pi^+\pi^-\pi^0$
8. Dalitz plot analysis of hadronic decay $\eta' \to \pi^+\pi^-\eta$
9. First observation of G-parity violating decay $\phi \to \pi^+\pi^-\eta$

[1] K. Nakamura et al. (Particle Data Group), J. Phys. **G37**, 075021 (2010).
[2] H. Fonvieille, N. Bensayah, J. Berthot, P. Bertin, M. Crouau, et al., Phys.Lett. **B233**, 65 (1989).
[3] F. Farzanpay, P. Gumplinger, A. Stetz, J. Poutissou, I. Blevis, et al., Phys.Lett. **B278**, 413 (1992).
[4] R. Meijer Drees et al. (SINDRUM-I Collaboration), Phys.Rev. **D45**, 1439 (1992).
[5] L. Landsberg, Phys.Rept. **128**, 301 (1985).
[6] H. Behrend et al. (CELLO Collaboration), Z.Phys. **C49**, 401 (1991).
[7] J. Gronberg et al. (CLEO Collaboration), Phys.Rev. **D57**, 33 (1998), hep-ex/9707031.
[8] B. Aubert et al. (BABAR Collaboration), Phys.Rev. **D80**, 052002 (2009), 0905.4778.
[9] H. N. Brown et al. ((Muon g-2 Collaboration)), Phys. Rev. Lett. **86**, 2227 (2001).
[10] H. Czyz, S. Ivashyn, A. Korchin, and O. Shekhovtsova (2012), 1202.1171.
[11] H. Berghauser, V. Metag, A. Starostin, P. Aguar-Bartolome, L. Akasoy, et al., Phys.Lett. **B701**, 562 (2011).
[12] R. Arnaldi et al. (NA60 Collaboration), Phys.Lett. **B677**, 260 (2009), 0902.2547.
[13] F. Stollenwerk, C. Hanhart, A. Kupsc, U.-G. Meissner, and A. Wirzba, Phys.Lett. **B707**, 184 (2012), 1108.2419.
[14] P. Adlarson et al. (WASA-at-COSY Collaboration), Phys.Lett. **B707**, 243 (2012), 1107.5277.
[15] M. Gormley, E. Hyman, W.-Y. Lee, T. Nash, J. Peoples, et al., Phys.Rev. **D2**, 501 (1970).
[16] A. Abele et al. (Crystal Barrel Collaboration), Phys.Lett. **B402**, 195 (1997).
[17] D. J. Gross, S. Treiman, and F. Wilczek, Phys.Rev. **D19**, 2188 (1979).
[18] M. Ablikim et al. (The BESIII), Phys. Rev. **D83**, 012003 (2011), 1012.1117.
[19] N. N. Achasov and A. A. Kozhevnikov, Int. J. Mod. Phys. **A7**, 4825 (1992).
[20] E. Abouzaid et al. (KTeV Collaboration), Phys.Rev. **D75**, 012004 (2007), hep-ex/0610072.
[21] A. E. Dorokhov and M. A. Ivanov, Phys.Rev. **D75**, 114007 (2007), 0704.3498.
[22] A. Dorokhov, M. Ivanov, and S. Kovalenko, Phys.Lett. **B677**, 145 (2009), 0903.4249.
[23] C. Terschlusen and S. Leupold, Phys.Lett. **B691**, 191 (2010), 1003.1030.
[24] R. Dzhelyadin, S. Golovkin, A. Konstantinov, V. Konstantinov, V. Kubarovsky, et al., Phys.Lett. **B102**, 296 (1981).